Production of UHPFRC nodes for timber structures in the Canadian West Coast: Lessons learned

Amr Abdallah[1[0000-0001-5211-5182]], MD Shahnewaz[2[0000-0002-3814-8508]], Carla Dickof[3[0000-0002-7484-8691]], and Lisa Tobber[4[0000-0003-1134-3335]]

[1] Postdoctoral research fellow, University of British Columbia Okanagan, Kelowna BC V1V1V7, Canada, Engineer intern, Fast + Epp, Vancouver BC V5Y1M2, Canada
[2] Research Manager, Fast + Epp, Vancouver BC V5Y1M2, Canada
[3] Associate Principal, Fast + Epp, Vancouver BC V5Y1M2, Canada
[4] Assistant professor at the School of Engineering, University of British Columbia Okanagan, Kelowna BC V1V1V7, Canada
amr.abdallah@ubc.ca, aabdallah@fastepp.com

Abstract. This paper introduces a novel precast ultra high-performance fibre-reinforced concrete (UHPFRC) nodes for mass timber post-and-beam gravity system. The details of casting of the UHPFRC specimens at a local precast concrete manufacturing plant in the lower mainland, BC, Canada, are discussed. In addition, extensive laboratory tests were performed on precast nodes at Fast + Epp's Concept Lab, Vancouver, Canada, and the outcomes are discussed. Fifteen precast UHPFRC nodes, representing column-corbel joints were cast and tested under monotonic loading. The tested variables were the width and depth of the corbels in addition to the presence of a lower column stub. The specimens were tested up to complete failure and the failure surfaces were closely examined. The test results exhibited significant variation in the load carrying capacity of the tested replicates, which can be attributed to the poor fibre orientation as observed within the failure surfaces of some specimens. Therefore, an improved manufacturing procedure for precast UHPFRC elements, over the typically followed ones for conventional precast concrete elements, has been recommended. This includes a few upgrades to the fabrication plant in addition to more controlled and specified roles for each personnel to ensure a more efficient process for the quality control of UHPFRC.

Keywords: Fibre-reinforced concrete, ultra high-performance fibre-reinforced concrete (UHPFRC), precast concrete, corbel, mass timber

1 Introduction

The current need for more housing and the negative impacts of global warming caused by conventional building materials have required the adoption of more sustainable structures [1]. Over the last two decades, the use of timber as a construction material has become more commonplace owing to its favorable properties. For instance, wood is renewable and can be sourced from sustainably managed forests. In addition, timber captures carbon, reducing the overall carbon footprint of the building. Furthermore, the engineered mass timber products have a high strength-to-weight ratio. Amongst such products, prefabricated timber panels can be used which allows for a faster and more efficient construction [2-3].

Due to the limitations of wooden structural systems, in terms of ductility and thermal and acoustic properties, the concept of hybrid structures has been proposed and implemented [4-6]. In these systems, timber constitutes the majority of the structure with structural steel or reinforced concrete (RC) seismic force-resisting systems (SFRS). An example of such a hybrid structure is the Brock Commons student residence hall at the University of British Columbia [7], which is the tallest timber building in Canada and was the tallest in the world at the time it was constructed. This structure included two RC core walls as the SFRS along with cross-laminated timber (CLT) panels and glulam columns comprising the gravity load-resisting frame (GLRF). An innovative hollow circular section (HCS) steel assembly was used at the CLT panel-column connections (Fig. 1).

(a) (b)

Fig. 1. Steel HCS connection for timber structures, (a) dismantled connection, and (b) A schematic sketch of the steel HSS connection joining CLT panels and Glulam columns (photos courtesy of Fast + Epp).

The utilized steel connections had some limitations which foster further research into other viable alternatives. For example, buildings typically require most structural elements to have up to 2-hour fire rating. While mass timber elements can provide the required fire rating through charring, the steel connections must be adequately fireproofed to meet this standard, which can be challenging. In addition, in post-and-beam timber structures, it could be inconvenient and time consuming to assemble the beam-column joint using the aforementioned column connection in addition to steel hangers to connect the beam ends to the columns.

To overcome the aforementioned issues, the use of precast ultra high-performance fibre-reinforced concrete (UHPFRC) nodes at the beam-column joints of the timber GLRF was proposed (Fig. 2a). To provide structural integrity, steel rods glued into the timber members can be post-installed into the PC nodes (Fig. 2b). The versatility of precast concrete, convenience of mass production, ease of assembly, and excellent fireproofing makes it a feasible solution [8-9]. In addition, the superior mechanical properties of UHPFRC enable the use of small-sized nodes with minimal or no steel bars or ties, which results in more convenient production and reduced labor. Furthermore, as a strong base material for the steel anchors, the use of UHPFRC may successfully accommodate the post-installed steel anchors with shallower embedment depths and smaller edge distance and spacing compared to those needed for conventional concrete [10-14].

This paper discusses the feasibility of this novel UHPFRC node in mass timber buildings. The paper highlights the procedure and lessons learned from the casting of UHPFRC node specimens at a local precast concrete manufacturing plant in the lower mainland of British Columbia, Canada. A summary of the tests conducted is provided and test observations and results are discussed. The observed failure patterns and load capacities suggested key recommendations for the implementation of UHPFRC at local precast concrete plants in the Canadian West Coast.

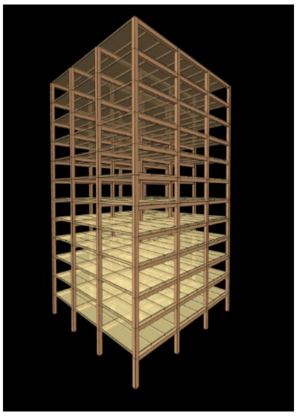

(a)

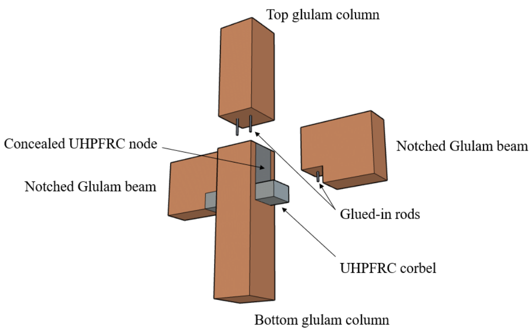

(b)

Fig. 2. An overview of the isolated beam-column joint, (a) general layout of the prototype structure (photo courtesy of Fast + Epp), and (b) isometric view of the precast concrete node and glulam beams and columns comprising the isolated joint.

2 Experimental Program

2.1 Properties and Mixing Procedure of the UHPFRC

A commercially available proprietary UHPFRC product, ce200SF-GTM, with a target 28-day compressive strength of the used UHPFRC of 130 MPa, was used to cast the specimens tested in this study. A white pre-blend mix (i.e., high-strength render (HSR) cement, finely graded sand, and other components), carbon nanofibres (CNF) paste, micro steel fibres at 2% volume fraction, along with potable water comprised the UHPFRC mix. Table 1 lists the mixing proportions of the used UHPFRC [15] The micro steel fibres (Fig. 3a) were straight with a 0.2-mm diameter, 13-mm length, and a 2850MPa tensile strength as per ASTM A820-22 [16].

Table 1. Mixing proportions of the UHPFRC [15]

Component	Ce200SF-G^{TM} premix	Steel fibres	cePAA1-80SDR[a]	Potable water
Quantity (kg/m^3)	2155.0	156.0	12.9	225.8

[a] Carbon nanofibers (CNF) paste

A high shear mixer with a 0.25 m3 capacity was used to perform the mixing (Fig. 3b), where the mixing procedure followed the recommendations of the supplier [15]. Prior to casting the specimens, the flow test was performed as per ASTM C1856 [17], where the average diameter was approximately 240 mm. The staff of the precast plant followed the typical precast practice, where each member of staff assisted with the casting in a dynamic manner, as applicable (Fig. 3c). This resulted in a somewhat inconsistent casting procedure in terms of casting point, height, position of the form-work, and the used receptacle. Moreover, occasional fibre balling was noticed during casting where some of such masses were taken out of the fresh UHPRC being cast, as much as possible (Fig. 3d). To evaluate the material properties of the hardened UHPFRC, axial compressive and flexural, tests were conducted on 75 × 150-mm cylinders, and 150 × 150 × 500-mm prisms, respectively, as per ASTM C1856 [17]. The mechanical properties of the hardened UHPFRC are listed in Table 2.

Table 2. Hardened properties of the UHPFRC

Material property	Compressive strength (MPa)[a]	Flexural strength (MPa)[a]
Value	130.6 $\pm$ 0.9	16.2 $\pm$ 0.7

[a] Performed as per the respective ASTM standards and ASTM C1856 [17].

(a) (b) (c) (d)

Fig. 3. Preparing the UHPFRC mixture, (a) steel fibres, (b) the used mixer, (c) pouring the UHPFRC nodes, and (d) fibre clumps removed

2.2 Specimen Details

Fifteen node specimens were cast using UHPFRC, including three identical replicates for each specimen of those listed in Table 3, to address the variation of the test results. No steel bars or stirrups were included to reduce the associated labor and/or cost and since some previous studies proved the efficiency of UHPFRC members and joints without longitudinal and/or transverse reinforcement [18-23]. The load-carrying capacity of the nodes was predicted using the model of Fattuhi et al. [24] and through a preliminary finite-element model (FEM) considering the expected mechanical properties of the UHPFRC [19], as listed in Table 3. The test specimens replicated the beam-column joints of a GLRF within an intermediate story of a hybrid RC-timber structure as shown in Fig. 2. In the prototype structure, the glulam beams are end-notched to create a smooth soffit when carried by the shallow UHPFRC corbel. In addition, the glulam beams were assumed to be in one direction only without transverse beams. The limited width of the UHPFRC nodes was proposed to suit the typical width of timber beams while allowing the node to be concealed within the mass timber columns, promoting a more aesthetic appearance.

The details of the tested specimens, as they were positioned in the test setup, are depicted in Fig. 4, where the first two specimens, S-100-100-150 and X-100-100-150, assessed the effect of the presence of the lower column stub (i.e., upper column stub as per the implemented test setup). The other tested parameters were the width and depth of the corbels, while the length of all corbels was 150 mm. A four-character alphanumeric code was utilized to identify the test specimens, where the first letter, S and X, indicated the presence or absence of the lower column stub, respectively. The second, third and fourth digits identified the width, thickness and length of the corbels, respectively. For example, the specimen S-100-100-150 was a UHPFRC node with a lower column stub and a 100-mm wide, 100-mm deep and 150-mm long corbel on either side.

Table 3. Properties of the UHPFRC node specimens

Specimen ID[a]	Presence of lower column stub	Width (mm)	Corbel thickness (mm)	Corbel length (mm)	Predicted load (kN)	
					Fattuhi et al. [24]	FEM
S100-100-150	Y	100	100	150	167	122
X100-100-150	N	100	100	150	167	122
X100-125-150		100	125	150	255	204
X100-100-100		100	100	100	238	183
X150-100-150		150	100	150	251	201

[a] Three identical replicates were cast and tested for each specimen.

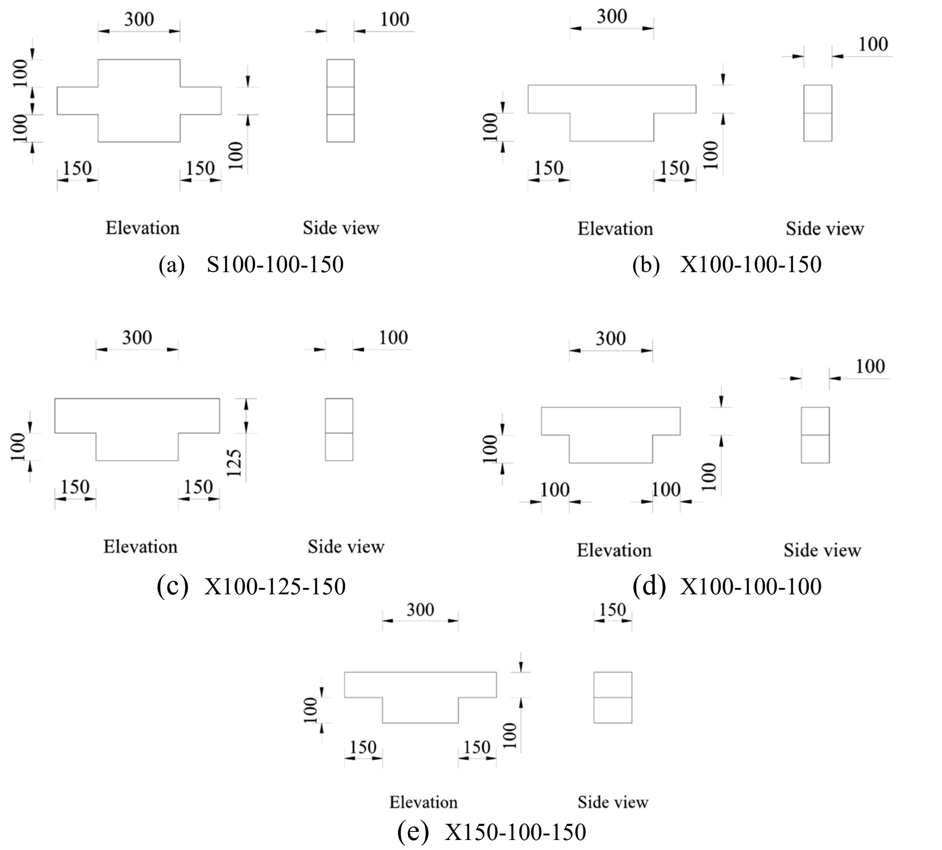

Fig. 4. Details of the UHPFRC node specimens, (a) S100-100-150, (b) X100-100-150, (c) X100-125-150, (d) X100-100-100, and (e) X150-100-150 (all dimensions in mm).

2.3 Test Setup and Procedure

The corbel tests were performed using a self-reacting steel frame, equipped with a 500-kN capacity hydraulic actuator. Following the available literature [19, 25], the test setup was prepared to depict an inverted configuration of the actual loading case, where the column reaction was applied through the actuator and the beam reactions (i.e., carried by the corbels) were represented in the test setup by the reactions of the corbels against the supporting pinned supports welded to the transverse steel beams below, as shown in Fig. 5. The pin supports were located at mid-length of each corbel.

The load was applied monotonically with a displacement-controlled rate of 0.25 mm/min up to failure, where the real-time load values were extracted from the built-in load cell of the actuator through a computerized data acquisition system (DAQ). In addition, two string potentiometers (SPs) were attached to the lower inner corner of the corbel on each face of the node to monitor the corbel deflection during the tests.

Fig. 5. Test setup and instrumentation for the UHPFRC.

3 Test Results and Discussion

Figure 6 shows the load-deflection responses of the tested node specimens. Generally, the response was linear up to about 90% of the peak load capacity. The relationships exhibited softening afterward until the load capacity of the corbels was reached, followed by a descending branch until failure. As expected, all specimens exhibited a single crack at the corner on the tension side of the corbel-column conjunction following the achievement of the peak load resistance. This crack propagated upwards as the loading continued, accompanied by degradation of the load resistance of the node. Examples of node specimens after testing are shown in Fig. 7. For specimens X100-100-150 and X100-100-100, the responses of two replicates only are shown as the third replicate for each was deemed an anomaly and excluded accordingly.

The load-carrying capacities of the tested nodes were between 40% and 73% of those predicted using either the model of Fattuhi et al. [24] or FEM. In addition, a significant variation was observed between the responses of the different replicates of the same specimen. Such results strongly indicate poor fibre orientation which can be attributed to the varied pouring points and casting styles in addition to the presence of fibre balling observed for some specimens.

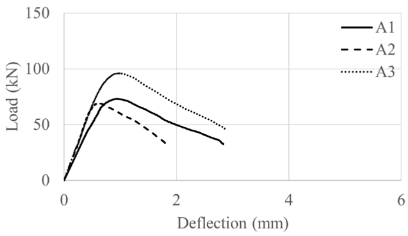

(a) S100-100-150

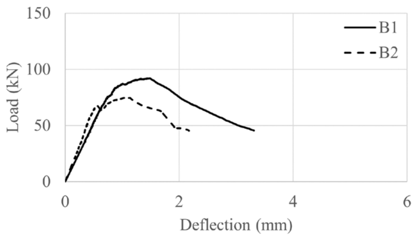

(b) X100-100-150

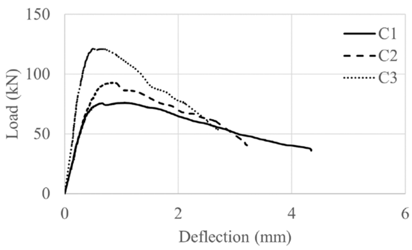

(c) X100-125-150

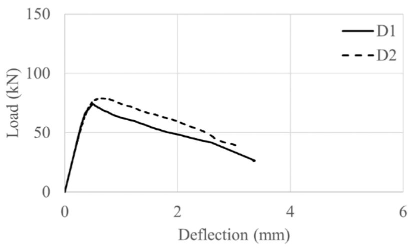

(d) X100-100-100

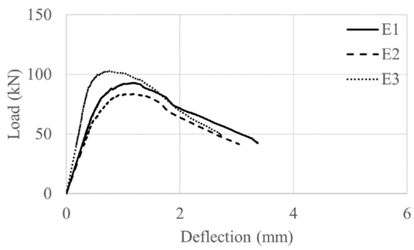

(e) X150-100-150

Fig. 6. Load-deflection responses of the UHPFRC node specimens, (a) S100-100-150, (b) X100-100-150, (c) X100-125-150, (d) X100-75-150, (e) X100-100-100, and (f) X150-100-150

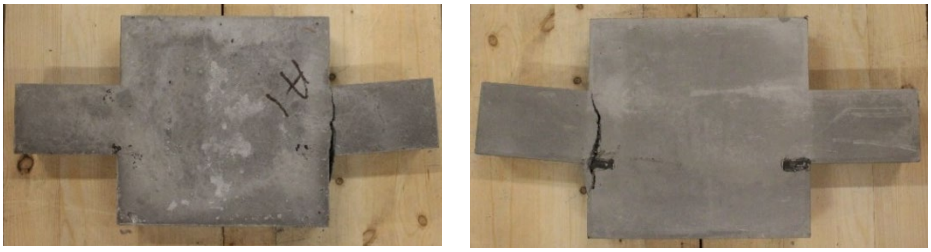

(a) S100-100-150

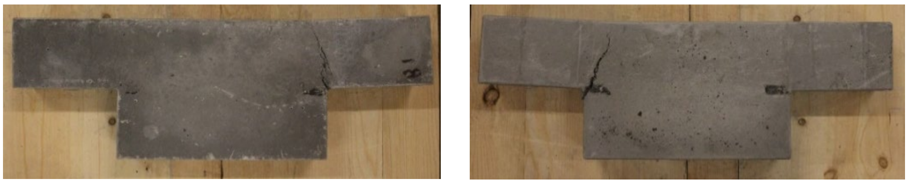

(b) X100-100-150

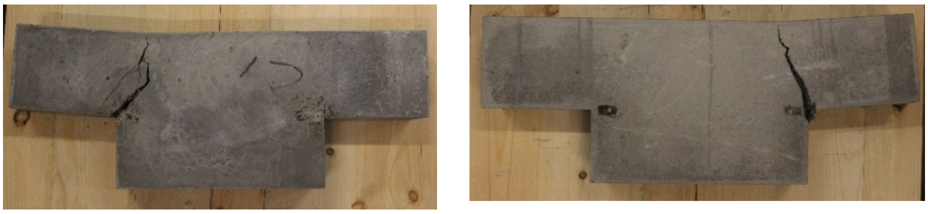

(c) X100-125-150

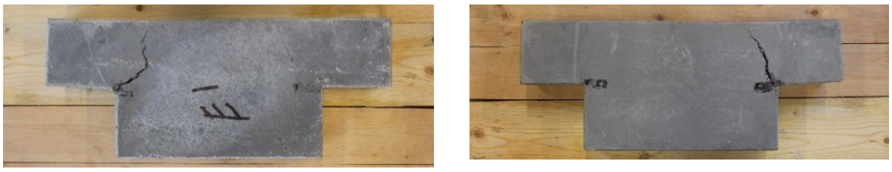

(d) X100-100-100

(e) X150-100-150

Fig. 7. Typical failures of UHPFRC node specimens (left photo: front face, right photo: back face).

Such observations required checking the failure surface of the node specimens and prisms, and their associated fibre orientation. As shown in Fig. 8, better dispersion of fibres can be observed for specimens A3 and C3 compared to their counterparts A2 and C1, respectively, where some spots across the cross-section lack the presence of fibres for the latter couple of nodes. This agrees well with the larger load capacity exhibited by A3 and C3 compared to their replicates, which indicates an issue with the mixing and/or pouring process for the tested specimens. These issues can be attributed to the lack of clarity on mixer speed during mixing by the supplier, fibre balling, the different casting styles executed by the different personnel at the precast plant for the different replicates with respect to casting point, the position of the formwork, and the used receptacles.

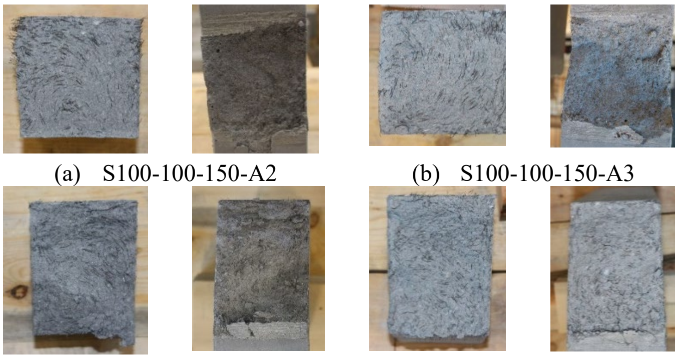

(a) S100-100-150-A2 (b) S100-100-150-A3

(c) X100-125-150-C1 (d) X100-125-150-C3

Fig. 8. Comparisons between the failure surfaces of UHPFRC node replicates

These issues were discussed with the supplier and the precaster and the following alterations were proposed: (1) specifying minimum mixer speed to approve the test facility for UHPC production, (2) using a removable steel-wire mesh door on top of the receptacle of the mixer to ensure better fibre dispersion during mixing, (3) specifying a role for each personnel during the pouring rather than the dynamic team configuration practiced during conventional precast concrete casting, (4) having improved training of personnel as per the available certification programs for UHPC production labor, (5) and specifying the casting point for each type of specimens ensuring consistent pouring.

4 Conclusions

Using ultra high-performance fibre-reinforced concrete (UHPFRC), node specimens were cast and tested to evaluate their use as precast beam-column joints for timber structures. Based on the test observations, the following conclusions can be drawn:

1. While the actual compressive strength achieved by the UHPFRC cylinders satisfied the target strengths for each mix, the achieved flexural strength was about 28% of

that specified in the datasheet of the used mixture. This indicates poor quality control, most likely due to fibre dispersion and orientation. This was corroborated by the observed fibre dispersion across the failure surface for the node and prism specimens.

2. The tested node specimens achieved lower load capacities compared to those theoretically or numerically predicted. Furthermore, significant variation between the results of the replicates of each specimen was observed, which was attributed to the variation in fibre-orientation.
3. The current test observations indicate issues with the production and casting of the UHPFRC. This can be attributed to the lack of clarity of mixer speed during mixing by the supplier, fibre balling, different casting style for the different specimens with respect to casting point, the position of the formwork, and the used receptacles. Such issues are expected to occur during any concrete pouring and reliable measures should be taken when producing such UHPFRC elements.

Acknowledgements

The authors would like to express their sincere gratitude to Mitacs Accelerate Fellowship and Fast + Epp Structural Engineers Ltd for their financial support. The technical assistance and facilities provided by the technical staff of the Concept Lab at Fast + Epp Structural Engineers Ltd and the University of British Columbia Okanagan are greatly appreciated. The UHPC and formwork were generously donated by Sanderson Concrete Inc. In addition, the technical advice provided by Mr. Vic Perry from ceEntek Pte Ltd before, during, and after casting the specimen is highly valued.

References

1. Tesfamariam, S., Skandalos, K., Goda, K., Bezabeh, M. A., Bitsuamlak, G., and Popovski, M. Quantifying the Ductility-Related Force Modification Factor for 10-Story Timber–RC Hybrid Building Using FEMA P695 Procedure and Considering the 2015 NBC Seismic Hazard. Journal of Structural Engineering, 147(5), 04021052 (2021).
2. Isoda, H., and Tesfamariam, S. Connections for Timber – Concrete Hybrid Building: Experimental and Numerical Model Results. J. Perform. Constr. Facil., 3(5), 04016024 (2016).
3. NRCan (Natural Resources Canada). “Canada investing to grow markets for B.C. wood products.” Accessed August 8, (2022).
4. Banks W.: Multi-storey timber construction—a feasibility study. NZ Timber Des J 8(2):14–23 (1999).
5. Hein C.: Developing hybrid timber construction for sustainable tall buildings. CTBUH J 3:40–45 (2014).
6. Isoda, H., Kawai, N., Koshihara, M., Araki, Y., and Tesfamariam, S. Timber – Reinforced Concrete Core Hybrid System: Shake Table Experimental Test. J. Struct. Eng., 143(1), 04016152 (2017).
7. Fast, P., Gafner, B., and Jackson, R. Eighteen Storey Hybrid Mass Timber Student Residence at the University of British Columbia Eighteen Storey Hybrid Mass Timber Student

Residence at the University of British Columbia. Structural Engineering International, 27(1), 44–48 (2018).

8. Hartig, J., Haller, P., and Heiduschke, A. Holzfachwerke mit Verbindungsknoten aus Beton: Teil 1: Konzept und experimentelle Untersuchungen. Bautechnik, 90(1), 1-8 (2013).
9. Negrão, J. H., Brito, L. D., Dias, A. G., Júnior, C. C., and Lahr, F. R. Numerical and experimental study of small-scale moment-resistant reinforced concrete joints for timber frames. Construction and Building Materials, 118, 89-103 (2016).
10. Cattaneo, S., and Muciaccia, G. Adhesive anchors in high performance concrete. Materials and Structures/Materiaux et Constructions, 49(7), 2689–2700 (2016).
11. Choi, S., Joh, C., and Chun, S. C. Behavior and strengths of single cast-in anchors in Ultra-High-Performance Fiber-Reinforced Concrete (UHPFRC) subjected to a monotonic tension or shear. KSCE Journal of Civil Engineering, 19(4), 964–973 (2015).
12. Delhomme, F., and Brun, M. Pullout simulation of post installed chemically bonded anchors in UHPFRC. MATEC Web of Conferences, 199 (2018).
13. Delhomme, F., and Brun, M. Pullout Tests on Post-installed Bonded Anchors in Ultra-high Performance Fiber Reinforced Concrete. Structural Engineering International, 29(3), 417–424 (2019).
14. Li, F., Tang, H., Wen, T., Li, J., Chen, Z., Jiang, Y., and Gao, H. Pullout behavior of studs in ultra-high performance concrete with steel fibers and novel structural fibers. Structures, 44, 405–417 (2022).
15. ceEntek Pte Ltd. "ce200SF-G™ —Technical data sheet." ceEntek Canada Ltd. Calgary, AB, Canada (2021).
16. ASTM A820/A820M-22, "Standard Specification for Steel Fibers for Fiber-Reinforced Concrete," ASTM International, West Conshohocken, PA, (2022).
17. ASTM C1856-17 A. Standard Practice for Fabricating and Testing Specimens of Ultra-high Performance Concrete, ASTM International, West Conshohocken, PA (2017).
18. Abdo, A., Mohamed, H. A., Ryad, T., and Ahmed, S. The impact of utilizing UHPFRC in beam-column joints with different patterns of transverse reinforcement. Frattura ed Integrità Strutturale, 17(64), 11-30 (2023).
19. Ridha, M. M., Al-Shafi'i, N. T., and Hasan, M. M. Ultra-high performance steel fibers concrete corbels: Experimental investigation. Case studies in construction materials, 7, 180-190 (2017).
20. Solhmirzaei, R., Kodur, V. K. R., and Banerji, S. Shear behavior of ultra high performance concrete beams without stirrups. In International Interactive Symposium on Ultra-High Performance Concrete (Vol. 2, No. 1). Iowa State University Digital Press (2019, June).
21. Yang, I. H., Joh, C., and Kim, B. S. Structural behavior of ultra high performance concrete beams subjected to bending. Engineering structures, 32(11), 3478-3487 (2010).
22. Zhang, Z. Y., Ding, R., Nie, X., and Fan, J. S. Seismic performance of a novel interior precast concrete beam-column joint using ultra-high performance concrete. Engineering Structures, 222, 111145 (2020).
23. Zhou, C., Wang, J., Jia, W., and Fang, Z. Torsional behavior of ultra-high performance concrete (UHPC) rectangular beams without steel reinforcement: Experimental investigation and theoretical analysis. Composite Structures, 299, 116022 (2022).
24. Fattuhi, N. I. Strength of FRC corbels in flexure. Journal of Structural Engineering, 120(2), 360-377 (1994).
25. Md Zin, N., Al-Fakih, A., Nikbakht, E., Teo, W., and Anwar Gad, M. Influence of secondary reinforcement on behaviour of corbels with various types of high-performance fiber-reinforced cementitious composites. Materials, 12(24), 4159 (2019).